Journal of Biomedical Optics

SPIEDigitalLibrary.org/jbo

Three-dimensional volumetric human meibomian gland investigation using polarization-sensitive optical coherence tomography

Myeong Jin Ju
Jun Geun Shin
Sujin Hoshi
Yoshiaki Yasuno
Byeong Ha Lee
Shuo Tang
Tae Joong Eom

Three-dimensional volumetric human meibomian gland investigation using polarization-sensitive optical coherence tomography

Myeong Jin Ju,[a,b] Jun Geun Shin,[c] Sujin Hoshi,[b,d] Yoshiaki Yasuno,[b] Byeong Ha Lee,[c] Shuo Tang,[a] and Tae Joong Eom[e,*]

[a]University of British Columbia, Department of Electrical and Computer Engineering, 2332 Main Mall, Vancouver, BC, V6T 1Z4, Canada
[b]University of Tsukuba, Institute of Applied Physics, Tennodai 1-1-1, Tsukuba, Ibaraki 305-8573, Japan
[c]Gwangju Institute of Science and Technology, School of Information and Communication, 123 Cheomdan-gwagiro, Gwangju 500-712, Republic of Korea
[d]University of Tsukuba, Faculty of Medicine, Department of Ophthalmology, Tennodai 1-1-1, Tsukuba, Ibaraki 305-8575, Japan
[e]Gwangju Institute of Science and Technology, Advanced Photonic Research Institute, 123 Cheomdan-gwagiro, Gwangju 500-712, Republic of Korea

Abstract. In this study, polarization-sensitive optical coherence tomography (PS-OCT) capable of providing polarization contrasts such as phase retardation and degree of polarization uniformity (DOPU) was used for visualizing human meibomian glands (MGs) and investigating morphological characteristics of them. Especially, with the help of the DOPU contrast, MGs were exclusively extracted from the volumetric OCT image. *In vivo* PS-OCT measurements were performed on the upper eyelids of different age groups. From these measurements, different age-dependent aspects of the MG structure were also observed. Based on these observations, it can be inferred that the PS-OCT system has the potential for clinical diagnosis and investigation of MG-related dry eye diseases like MG dysfunction (MGD) and acinar atrophy. [DOI: 10.1117/1.JBO.19.3.030503]

Keywords: meibomian glands; optical coherence tomography; polarization-sensitive optical coherence tomography; medical imaging; biomedical optics.

Paper 130895LR received Dec. 19, 2013; revised manuscript received Jan. 27, 2014; accepted for publication Feb. 5, 2014; published online Mar. 6, 2014.

Human meibomian glands (MGs) are large secretory lipid-excreting glands embedded in a tarsal plate with approximately 31 and 26 individual glands in the upper and the lower eyelids, respectively.[1] Each MG comprises multiple acini that are circularly arranged around a common central duct and connected to it by a short ductle. A single acinus having an elongated or spherical shape of about 150 to 200-μm diameter is completely filled with secretory cells termed meibocytes.[2] Meibum, the oily secretory product from the meibocyte, is the main component of the superficial layer of the tear film and has important functions such as the formation of a hydrophobic barrier to prevent the tear overflow onto the lids[2] and the stabilization of the tear film by lowering surface tension.[3] Importantly, the meibum may also provide a barrier to prevent the entry of bacteria into the tear film and inhibit the entry of undesirable sebum at the lid margin.[2]

As the interests in MG functions grow, several imaging modalities have been developed for visualization and investigation of the MGs and utilized for the diagnosis of the MG-related diseases [e.g., MG dysfunction (MGD)]. In a recent study by Ngo et al.,[4] functionalities and characteristics of several MG visualization methods such as lid transillumination, video and noncontact meibography, confocal microscopy, ultrasound, and optical coherence tomography (OCT) were comprehensively provided. Owing to its capability of creating volumetric structure in a noninvasive way and with high contrast and resolution, OCT has been most recently utilized for visualizing the MGs.[5,6] In the study,[6] in order to investigate the morphological alternation of the MGs followed by different pathological conditions, *in vivo* three-dimensional (3-D)-OCT imaging was performed on the upper eyelid of subjects with normal MGs, MGD, and dry eye disease. For extracting a volumetric MG structure, the palpebral conjunctiva layer above the MGs was arbitrarily cropped out by the examiner from the scattering OCT intensity contrast. However, the accuracy of the differentiation between the conjunctiva layer and the MGs was not guaranteed because of the absence of any specific criteria for MG classification. Furthermore, due to the limited imaging range of 5×2 mm^2, it seems to be difficult for observing the overall feature of the MG structure and for assessing the MG dropout (disappearance of the glandular tissue inside the tarsal plate). To our knowledge, for the first time, we demonstrate the functionality of polarization-sensitive OCT (PS-OCT) in terms of the visualization and investigation of MGs.

A Jones matrix–based PS-OCT system, whose technical details are described in Ref. 7, was employed in this study. The system is based on a high-speed scanning laser (HSL-2000, Santec Corp., Komaki, Aichi) with 30-kHz sweeping rate and a center wavelength of 1.31 μm. It consists of optical fiber–based Mach–Zehnder interferometer, electro-optic modulator (PC-B3-00-SFAP-SFA-130-UL, EOspace, Redmond, Washington) for continuous polarization modulation of the light source along the wavelength sweeping, and two balanced photodetectors (BPD-200, Santec Corp.) used for polarization diversity (PD) detection of both vertically polarized and horizontally polarized spectral interferograms. The probing power was measured to be 2.8 mW, which is below the laser safety limits prescribed by American National Standard Institute. The axial resolution and depth range of the system were measured to be around 12.7 μm (in air) and 5.3 mm, respectively. However, practical imaging depth from the surface of the palpebral conjunctiva to the MGs was limited to about 1.2 mm. From the center of the upper eyelid shown in Fig. 1(a), the 3-D-OCT volumetric image covering the transversal area of 10×10 mm^2 [512 (horizontal) $\times$ 256 (vertical) A-lines] with lateral resolution of 20.5 μm (in air) was obtained in 5.4 s.

*Address all correspondence to: Tae Joong Eom, E-mail: eomtj@gist.ac.kr

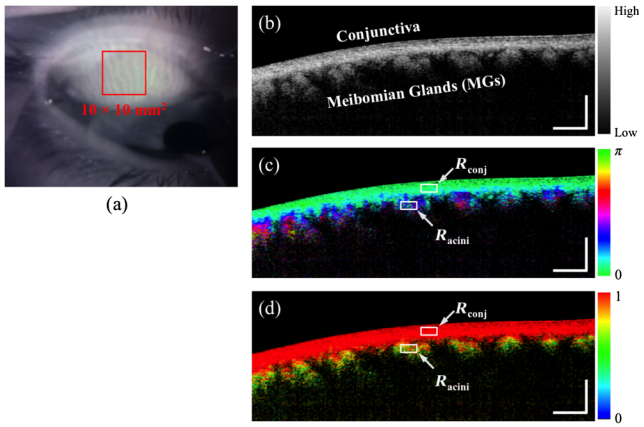

Fig. 1 Meibography image (a) and polarization-sensitive optical coherence tomography (PS-OCT) cross-sectional images: (b) scattering intensity OCT image, (c) phase retardation image, and (d) DOPU image. The scale bar represents 1×1 mm^2.

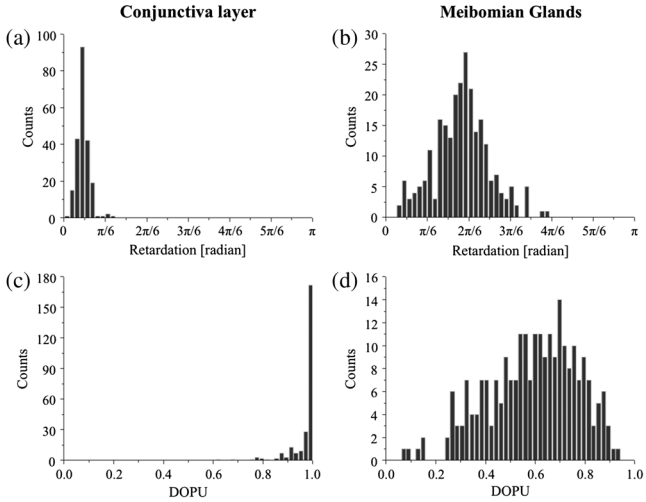

Fig. 2 Histograms of retardation and degree of polarization uniformity (DOPU). (a, c) Data from R_{conj} and (b, d) data from R_{acini} in Figs. 1(c) and 1(d).

By employing sinusoidal incident polarization modulation and the PD detection, interference signals of two different polarization states are detected simultaneously. From the obtained interferograms, four OCT signals corresponding to the Jones matrix elements are extracted and then processed by the Jones matrix analysis algorithm.[8–10] In the algorithm, the global phase compensation and the complex moving average processes are supplemented in order to create the phase retardation image with improved signal-to-noise ratio and image quality.[7] In addition to the phase retardation image, degree of polarization uniformity (DOPU)[11] contrast image is also acquired from the averaged Jones matrix.[12] Here, for both the complex moving averaging and the DOPU calculations, spatial kernel size of 5 pixels × 3 pixels (horizontal × depth) is applied.

Figure 1 shows the representative cross-sectional PS-OCT images [Figs. 1(b)–1(d)] obtained within the red window in the meibography image [Fig. 1(a)]. The meibography image is captured by IR-CCD camera and exhibits a wide range of gland morphology. From the cross-sectional scattering OCT image [Fig. 1(b)], the conjunctiva layer and the MGs can be roughly identified by different intensity contrasts. The conjunctiva layer appearing as hyperscattering in the OCT image shows nearly constant value in the phase retardation image [Fig. 1(c)] and the value close to 1 in the DOPU image [Fig. 1(d)]. In contrast with the conjunctiva layer, nonconstant retardation and relatively lower DOPU quantities are observed from the MGs, as shown in Figs. 1(c) and 1(d).

In this study, histogram-based polarization contrast analysis was performed for acquiring the criteria to make a discrimination between the conjunctiva layer and the MGs. Based on the criteria, it can be expected to achieve more reliable volumetric MG structure investigation. The representative regions within the conjunctiva layer and the acini (R_{conj} and R_{acini}) were first selected as shown in Figs. 1(c) and 1(d). The histograms of the phase retardation and the DOPU quantities within the given area were then obtained as shown in Fig. 2.

In the R_{conj}, polarization-maintaining property of the layer is evident from the narrow width of the retardation histogram [Fig. 2(a)] with the standard deviation (SD) of 0.07 (in radian). On the contrary, in the case of the R_{acini} [Fig. 2(b)], the broad-phase retardation distribution represented by the histogram with the SD of 0.33 (in radian) is observed. Figures 2(c) and 2(d) show the DOPU histograms of the R_{conj} and the R_{acini}, in which the difference between the conjunctiva layer and the MGs is more clearly identified. Most pixels within the R_{conj} have the DOPU quantities higher than 0.95, whereas the DOPU values from the R_{acini} spread out over the DOPU range below the value of 0.95. This implies that the spatial uniformity of polarization within the conjunctiva layer is very high as compared with the one in the acini. As a result, the DOPU value of 0.95 was empirically set as the threshold for MG structure extraction.

Figure 3 illustrates the overall processing steps proposed in this research. In the 3-D volumetric OCT intensity image shown in Fig. 3(a), the conjunctiva layer and MGs appear with different intensities. On the other hand, the conjunctiva layer and MGs are displayed by red and green colors in Fig. 3(b), respectively. Here, red and green represent the regions over and below the DOPU threshold, respectively. After differentiating each region based on the threshold, the conjunctiva layer was segmented and applied to the OCT image as a binary mask. As a result, exclusive visualization of MG structure was achieved as shown in Fig. 3(c).

To demonstrate the clinical potential of the proposed method, age-dependent MG alteration was investigated as one of the clinical applications. For this purpose, six upper eyelids without dry eye disease and MGD disorder from six subjects of different ages were involved in this study.

Figure 4 shows the extracted 3-D volumetric MG structures obtained from the subjects: (a) 28 years, (b) 32 years, (c) 56 years, (d) 63 years, (e) 72 years, and (f) 82 years olds. In Figs. 4(a) and 4(b), round-shaped and well-arranged multiple acini are clearly observed. However, in Fig. 4(c), noticeable gland dropout process starts to appear at the bottom of the image, even though several MG branch still remain intact at the top. This decreasing number of active glands is considered as one of the evidences of a natural aging process on the lid. In addition, the MG structure with small and irregular shape is also found in Fig. 4(d). Unlike the other cases, most of the acini are not recognizable anymore in Figs. 4(e) and 4(f), instead randomly distributed thread-shaped structures are observed.

In summary, distinctive polarization features of the conjunctiva layer and the MGs were investigated by using the PS-OCT

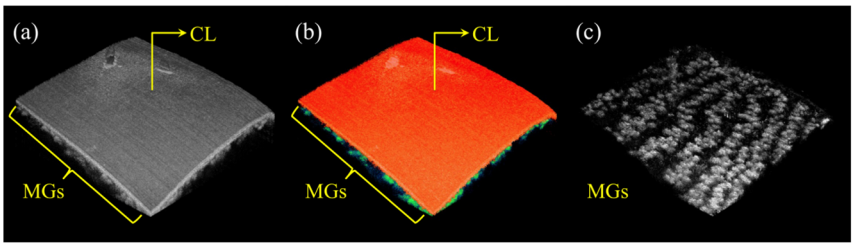

Fig. 3 Three-dimensional (3-D) vloume images: (a) original scattering OCT volume image, (b) classification-processed volume image, and (c) extracted MG volume image. In the processed volume image (b), red and green color regions represetent the conjunctiva layer (CL) and the meibomian glands (MGs), respectively.

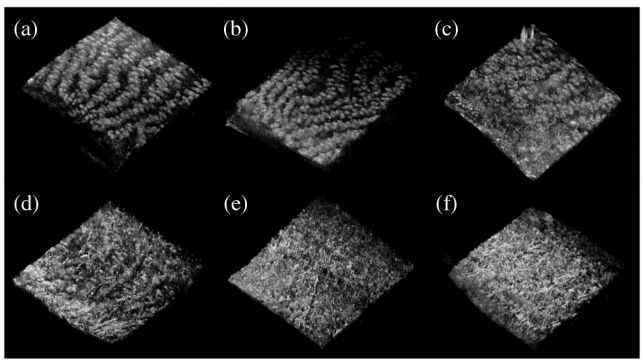

Fig. 4 Extracted MG volume structure images from the subjects: (a) 28 years, (b) 32 years, (c) 56 years, (d) 63 years, (e) 72 years, and (f) 82 years olds.

system. From the DOPU contrast, the discrimination criteria were empirically determined as the DOPU threshold. Using the threshold, segmentation of the conjunctiva layer and exclusive visualization of the MG structure were successfully achieved. In addition, age-dependent MG structure variation was also observed through *in vivo* measurements of several subjects with different ages, which demonstrates the clinical utility of the system for monitoring MG alteration and diagnosis of MG-related dry eye disease.

Acknowledgments

Myeong Jin Ju is supported by a University of British Columbia (UBC) Four Year Fellowship. This work was partially supported by the Technology Innovation Program funded by the Ministry of Trade, Industry & Energy (MI, Korea) (Grant No. 10040121) and the R&D innovation cluster development program of the Ministry of Science, ICT & Future Planning.

References

1. J. V. Greiner et al., "Volume of the human and rabbit meibomian gland system," *Adv. Exp. Med. Biol.* **438**, 339–343 (1998).
2. N. Nicolaides et al., "Meibomian gland studies: comparison of steer and human lipids," *Invest. Ophthalmol. Vis. Sci.* **20**(4), 522–536 (1981).
3. A. J. Bron et al., "Functional aspects of the tear film lipid layer," *Exp. Eye Res.* **78**(3), 347–360 (2004).
4. W. Ngo et al., "Historical overview of imaging the meibomian glands," *J. Optom.* **6**(1), 1–8 (2013).
5. K. Bizheva et al., "In vivo volumetric imaging of the human upper eyelid with ultrahigh-resolution optical coherence tomography," *J. Biomed. Opt.* **15**(4), 040508 (2010).
6. H. S. Hwang et al., "In vivo 3D meibography of the human eyelid using real time imaging Fourier-domain OCT," *PLoS ONE* **8**(6), e67143 (2013).
7. Y. Lim et al., "Birefringence measurement of cornea and anterior segment by office-based polarization-sensitive optical coherence tomography," *Biomed. Opt. Express* **2**(8), 2392–2402 (2011).
8. M. Yamanari et al., "Polarization-sensitive swept-source optical coherence tomography with continuous source polarization modulation," *Opt. Express* **16**(8), 5892–5906 (2008).
9. B. H. Park et al., "Jones matrix analysis for a polarization-sensitive optical coherence tomography system using fiber-optic components," *Opt. Lett.* **29**(21), 2512–2514 (2004).
10. M. Yamanari et al., "Fiber-based polarization-sensitive Fourier domain optical coherence tomography using B-scan-oriented polarization modulation method," *Opt. Express* **14**(14), 6502–6515 (2006).
11. E. Götzinger et al., "Retinal pigment epithelium segmentation by polarization sensitive optical coherence tomography," *Opt. Express* **16**(21), 16410–16422 (2008).
12. M. J. Ju et al., "Advanced multi-contrast Jones matrix optical coherence tomography for Doppler and polarization sensitive imaging," *Opt. Express* **21**(16), 19412–19436 (2013).